NJC

Accepted Manuscript

This is an *Accepted Manuscript*, which has been through the Royal Society of Chemistry peer review process and has been accepted for publication.

Accepted Manuscripts are published online shortly after acceptance, before technical editing, formatting and proof reading. Using this free service, authors can make their results available to the community, in citable form, before we publish the edited article. We will replace this *Accepted Manuscript* with the edited and formatted *Advance Article* as soon as it is available.

You can find more information about *Accepted Manuscripts* in the Information for Authors.

Please note that technical editing may introduce minor changes to the text and/or graphics, which may alter content. The journal's standard Terms & Conditions and the Ethical guidelines still apply. In no event shall the Royal Society of Chemistry be held responsible for any errors or omissions in this *Accepted Manuscript* or any consequences arising from the use of any information it contains.

ROYAL SOCIETY OF CHEMISTRY

www.rsc.org/njc

Cite this: DOI: 10.1039/c0xx00000x

www.rsc.org/xxxxxx

ARTICLE TYPE

Synthesis of visible-light active V_2O_5/g-C_3N_4 heterojunction as an efficient photocatalytic and photoelectrochemical performance

Theerthagiri Jayaraman[a], Senthil Arumugam Raja[a], Annamalai Priya [a], Madhavan Jagannathan[a,*], MuthupandianAshokkumar[b]

Received (in XXX, XXX) XthXXXXXXXXX 20XX, Accepted Xth XXXXXXXXX 20XX
DOI: 10.1039/b000000x

A new V_2O_5/g-C_3N_4 nanocomposite was synthesized via wet impregnation method using V_2O_5 and g-C_3N_4, obtained from citric acid and urea. The phase purity, crystallite size and strain were ascertained by powder x-ray diffraction (XRD) analysis. Further, the synthesized photocatalysts were characterized by Fourier transform infrared spectroscopy (FT-IR), scanning electron microscopy (SEM), energy dispersive x-ray spectroscopy (EDAX), high-resolution transmission electron microscopy (HRTEM), UV-vis diffuse reflection spectroscopy (DRS) and photoluminescence spectroscopy (PL). The efficiency of the photocatalysts was evaluated from the photodegradation of direct red 81 (DR81), a target textile pollutant, under visible light irradiation. The photocatalytic experiments demonstrated that the V_2O_5/g-C_3N_4 composites showed much better photocatalytic degradability of DR81 than bulk V_2O_5 and g-C_3N_4, when used individually. The enhancement of photocatalytic degradation is attributed to the efficient charge carrier separation of photogenerated electron-hole pairs. PL and electrochemical impedance spectroscopic (EIS) results also support the above statement. Different mole% ratios (1, 2 and 3%) of V_2O_5 loaded composites have been prepared and 1% loaded composite was found to show optimal efficiency. A possible mechanism has been proposed for the photocatalytic degradation using V_2O_5/g-C_3N_4.

1. Introduction

Visible-light driven semiconductor based photocatalytic materials have drawn immense attention due to their potential applications in the photodegradation of organic and inorganic pollutants, fuel and hydrogen production.[1-6] Various semiconductor materials such as metal oxides, sulphides and oxynitrides have been identified as efficient photocatalysts for the degradation of toxic pollutants in water.[7-11] Titanium oxide (TiO_2) is one of the most widely studied materials for the degradation of organic pollutants in water because of its photostability, insolubility and non-toxicity. TiO_2 is more effective only under UV light, which limits its practical applications.[12-13] Therefore, enormous efforts have been made for the development of alternate visible light active photocatalysts for pollutant degradation.

Very recently, graphitic carbon nitride (g-C_3N_4) has shown great promise as a novel metal-free visible light photocatalyst due to its unique features, such as high chemical and thermal stability, appealing electronic and optical structures, and an appropriate band gap to absorb visible light.[14,15] Nevertheless, the photocatalytic activity of g-C_3N_4 is limited due to the high recombination rate of photoinduced electron-hole pairs and poor quantum yield.[16] In order to improve its photocatalytic performance several strategies have been adopted such as doping of metals[17], combining with other semiconductors to form a composite photocatalysts[18,19] and sensitizing with organic dyes.[20] Among these, coupling with other semiconductor materials is considered as the most efficient modification. The composite photocatalysts are shown to possess rapid charge carrier separation, thereby reducing the recombination of electron-hole pairs leading to enhanced photocatalytic efficiency. A variety of composite photocatalysts have been reported, for example, Ji et al.[21] have developed g–C_3N_4/$BiVO_4$ composite with enhanced visible light photocatalytic activity for the degradation of Rhodamine B. Chen et al.[22] have prepared g-C_3N_4-WO_3 composite photocatalyst by ball milling method and reported high photocatalytic activity for the degradation of methylene blue. Jiang et al.[23] have developed Ag_2S modified g-C_3N_4 (Ag_2S/g-C_3N_4) composite photocatalyst and employed for the photocatalytic H_2-production. All reports suggest that g-C_3N_4 composites are highly photocatalytic than bulk g-C_3N_4.

In the present investigation, we report on the synthesis of vanadium pentoxide (V_2O_5) - g-C_3N_4 nanocomposite photocatalysts by wet impregnation method. Urea was chosen as a precursor for synthesis of g-C_3N_4 because it is a low cost raw material. Citrate precursor route was employed to obtain V_2O_5,which is active in the visible region of the solar spectrum and also possess a narrow band gap.[24] The synthesized photocatalysts were characterized by powder XRD, FT-IR, SEM, EDAX, DRS and PL studies. The photoelectrochemical and photoctalytic activities were evaluated for the photodegradation of DR81 under visible light irradiation. Direct red 81 (DR81) was chosen for this study due to its harmful nature. DR81 is commonly used in textiles, leather, plastics and cosmetics industries to colour their products. The textile industry effluent carries large volume of wastewater with colored dyes and other additives which are highly toxic to the environment. A possible mechanism for the photodegradation process over V_2O_5/g-C_3N_4 composite has been proposed.

2. Experimental section

2.1 Materials

Ammonium vanadate (NH_4VO_3) and citric acid were purchased from Rankem India. Urea, Triton X-100, sodium sulphate and methanol were obtained from SDFCL India. Deionised water was obtained from Nice chemicals India and used for all the experiments. Direct red 81 was purchased from Sigma-Aldrich (Cat. no.195251). All reagents were of analytical grade and were used without further purification.

2.2 Synthesis of photocatalysts

Vanadium pentoxide (V_2O_5) was synthesized using NH_4VO_3 and citric acid. NH_4VO_3 and citric acid (1:3 mole ratio) were dissolved in deionised water and the resulting solution was continuously stirred to make homogeneous solution. The homogeneous solution was heated at 80 ^{0}C on a hot plate to obtain the vanadium-citrate precursor powder. The obtained precursor sample was calcined at 450 ^{0}C for 3 hours to get pure V_2O_5. The graphitic carbon nitride (g-C_3N_4) was prepared by thermal polycondensation of urea. In a typical synthesis, 9 g of urea was loaded in an alumina crucible with a cover to prevent sublimation of precursors and heated to 520 ^{0}C for 2 hours at heating ramp of 15 ^{0} C/min and the furnace was cooled to room temperature naturally. The yellow colored product was collected and ground to a powder.

The V_2O_5/g-C_3N_4 nanocomposite photocatalysts with different loading of V_2O_5 were synthesized using the following procedure: 0.5 g of g-C_3N_4 and different mole ratios 1%, 2% and 3% of V_2O_5 were added to 40 mL of methanol in a beaker. Then, the beaker was placed in an ultrasonic bath for 15 min and then it was vigorously stirred at 80 ^{0}C to obtain the powder composite photocatalysts. The obtained product after evaporation of the methanol was annealed at 300 ^{0}C for 30 min. The V_2O_5/g-C_3N_4 composites with different mole ratios 1%, 2% and 3% of V_2O_5 have been denoted in this manuscript as VOCN-1, VOCN-2 and VOCN-3, respectively.

2.3 Characterization of photocatalysts

The x-ray diffraction (XRD) patterns were recorded using a powder X-ray diffractometer (Mini Flex II, Japan) with Cu Kα radiation (λ= 0.154 nm) at a scan speed of 3^0/min. The phase purity was ascertained using x-ray diffraction. The crystalline size was analyzed using Scherrer's equation, $d=0.9\lambda/B\cos\theta$, where d is the crystallite size, λ is the wavelength of x-ray radiation, B is the full width half maximum value (FWHM) in radian and θ is the diffraction angle. The micro-strain (ε) of the photocatalysts were estimated using the $\varepsilon = B/4\tan\theta$ equation. Fourier transform infrared (FT-IR) spectra were recorded in the wavenumber range, 4000-600 cm^{-1} using an FT-IR (JASCO 460 plus) instrument. KBr was used as a reference for FT-IR analysis. The morphology of the products was examined by scanning electron microscopy (SEM) VEGA3TESCAN model. Elemental analysis was examined by using EDAX-Bruker Nano GmbH, X Flash Detector (Model-5010). The high-resolution transmission electron microscope measurements were conducted on a JEOL JEM-3010 electron microscope at 200 kV. UV-visible diffuse reflectance spectra of the samples were recorded using a Shimadzu 2100 UV-vis spectrophotometer in the range of 200-800 nm. $BaSO_4$ was used as the reference. The photoluminescence (PL) measurements were recorded at room temperature using Jobin Yvon Flurolog-3-11 spectroflurometer.

2.4 Photocatalytic activity

The photocatalytic performance of the synthesized V_2O_5/g-C_3N_4 composites were evaluated by the photodegradation of direct red 81 (DR81) under visible light irradiation. The visible light was provided by a 100 W tungsten halogen lamp. In each experiment, known amounts of photocatalysts were mixed with 75 mL of $5x10^{-5}$ M solution of DR81. Prior to the irradiation, the suspension was magnetically stirred in the dark for 120 min to reach adsorption-desorption equilibrium. During irradiation, 4 mL of aliquots were collected at fixed time intervals and filtered through a 0.45 µm membrane filter (Pall Corporation) to remove the photocatalyst particles. The concentration of aqueous DR81 was monitored by its absorbance at 563 nm using a Shimadzu UV-2450 spectrophotometer.

2.4 Photoelectrochemical studies

Photoelectrochemical measurements were carried out on a CHI608E electrochemical workstation. A 100 W Xe arc lamp (OSRAM, Germany) was used as the light source. A standard three electrode cell, with a Pt-wire as counter electrode, Ag/AgCl (in saturated KCl) as a reference electrode and the composite material as working electrode was used. An aqueous solution of 0.1 M Na_2SO_4 was used as an electrolyte. The working electrode was prepared using the following procedure. 5 mg of photocatalyst was ground with 10 µL of Triton X-100 and 20 µL of deionised water to make a slurry. The slurry was spread on a 2.5x2.5 cm^2 fluorine-doped tinoxide (FTO) glass substrate with an active area of about 0.75 cm^2 by doctor blade method using scotch tape as spacer and then dried in hot plate for overnight.

3. Results and Discussion

3.1 X-ray diffraction studies

The V_2O_5 and g-C_3N_4 were synthesized by the citric acid and urea precursor route. The V_2O_5/g-C_3N_4 nanocomposites were synthesized by wet impregnation method using V_2O_5 and g-C_3N_4.The x-ray diffraction (XRD) patterns of the synthesized V_2O_5, g-C_3N_4 and V_2O_5/g-C_3N_4 composites are shown in Fig. 1. The XRD of V_2O_5 exhibited several diffraction peaks corresponding to 2θ values of 15.3^0, 20.2^0, 21.5^0, 26.1^0,30.9^0, 32.3^0,37.2^0, 41.2^0, 45.5^0, 47.4^0 and 51.1^0. These peaks are attributed to the 200, 010, 110, 101, 310, 011, 301, 020, 411, 600 and 022 planes of an orthorhombic V_2O_5 (JCPDS card no.89-2483) and these are in good agreement with an earlier report by Gao et al.[25] In the case of g-C_3N_4, two distinct diffraction peaks are observed at 2θ=13. 06^0 and 27.42^0 which are indicated to the (100) and (002) planes of hexagonal graphitic carbon nitride [JCPDS card no.87-1526]. Also, the diffraction peaks at 27.42^0 and 13.04^0 correspond to the in-plane structural peaking motif and inter layer stacking of aromatic segments of g-C_3N_4.[26] However, both hexagonal phase of g-C_3N_4 and orthorhombic phase of V_2O_5 are observed in V_2O_5/g-C_3N_4 composite. Also, it can be seen that the peak intensity of V_2O_5 increases with an increase in V_2O_5 content, whereas the peak intensity of g-C_3N_4 decreases. The crystalline size and micro-strain of the V_2O_5, g-C_3N_4 and V_2O_5/g-C_3N_4 composites are calculated and summarized in Table 1. It can be observed that the average crystalline size of the V_2O_5/g-C_3N_4 composite is decreased while adding V_2O_5 to g-C_3N_4 and the micro-strain value is constant (~0.042) for V_2O_5/g-C_3N_4 which indicates that there is no variations in the crystalline structure of V_2O_5/g-C_3N_4 composites.

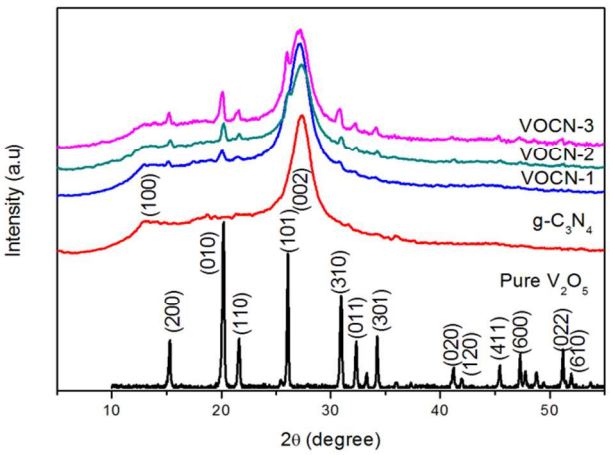

Fig. 1 XRD patterns of the synthesized V_2O_5, g-C_3N_4 and V_2O_5/g-C_3N_4 composite photocatalysts.

3.2 Fourier transform infrared studies

FT-IR spectra of the synthesized photocatalysts V_2O_5, g-C_3N_4 and V_2O_5/g-C_3N_4 are shown in Fig. 2. Two characteristic absorption bands at 824 cm^{-1} and 1014 cm^{-1} are observed in V_2O_5 sample. The band at 824 cm^{-1} is assigned to the asymmetric stretching modes of V-O-V bond and other peak at 1014 cm^{-1} is attributed to the stretching vibration of V=O bond.[27] Pure g-C_3N_4 shows strong band in the range of 3100-3300 cm^{-1}, which could be assigned to the stretching modes of N-H bonds of (-NH_3 and =N-H) amines.[28] The broad peaks in the range of 1200-1680 cm^{-1} are assigned to the stretching vibration modes of C=N and aromatic C-N heterocycles.[12] The absorbed peak at 812 cm^{-1} is attributed to the characteristic ring breathing mode of triazine units. Further, the FT-IR spectra of V_2O_5/g-C_3N_4 composites represent the overlap of the V_2O_5 and g-C_3N_4 spectra. The FT-IR peak intensity of g-C_3N_4 is decreased with increase in the mole percent of V_2O_5. This indicates the coexistence of the V_2O_5 and g-C_3N_4 in the composite and the XRD results also support this structure.

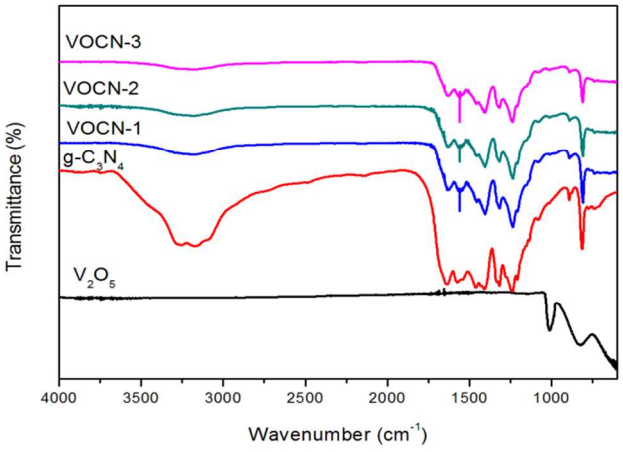

Fig. 2 FT-IR spectra of V_2O_5, g-C_3N_4 and V_2O_5/g-C_3N_4 photocatalysts.

Table 1 Crystalline size, micro-strain and band gap of synthesized materials

Sample	FWHM	Crystalline size (nm)	Micro-strain	Band gap (eV)
V_2O_5	0.221	36.53	0.005	2.33
g-C_3N_4	2.031	4.02	0.036	2.80
VOCN-1	2.321	3.52	0.042	2.69
VOCN-2	2.374	3.44	0.042	2.76
VOCN-3	2.341	3.49	0.042	2.81

3.3 Optical absorption studies

The optical properties of the composites were measured by using UV-visible diffuse reflectance spectroscopy and the results are shown in Fig. 3. The corresponding band gaps of the synthesized photocatalysts are listed in Table 1. The corresponding band gap energies of pure g-C_3N_4 and V_2O_5 are 2.80 and 2.33 eV, respectively. The absorption edges of V_2O_5 added g-C_3N_4 composites are significantly improved in the visible region after V_2O_5 loading, which may be due to the presence of a lower bandgap semiconductor.[29] The red shift in absorption edges of V_2O_5/g-C_3N_4 composite by the addition of V_2O_5 may contribute to the enhancement of photocatalytic activity of the composite samples under visible light irradiation.

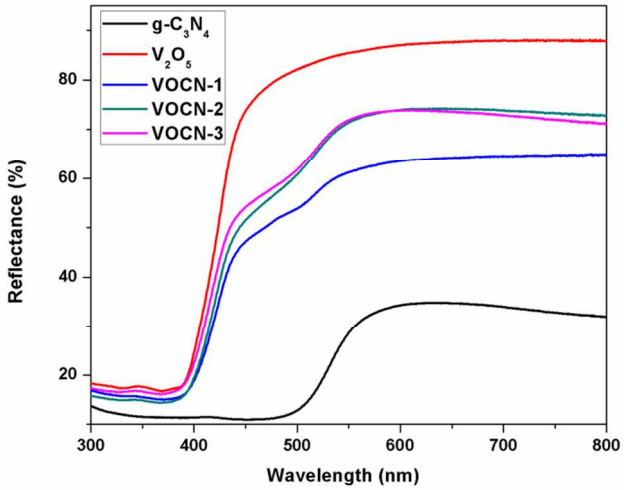

Fig. 3 UV-vis diffuse reflectance spectra of V_2O_5, g-C_3N_4 and V_2O_5/g-C_3N_4 composites.

3.4 Morphology and elemental studies

The morphology of the g-C_3N_4, $V_2O_5$and VOCN-1 were investigated by SEM analysis. The typical SEM photographs of V_2O_5, g-C_3N_4 and VOCN-1 are presented in Fig. 4(a), (b) and (c), respectively. Pure V_2O_5 sample shows a series of particles with stacked-up flakes like morphology whereas pure g-C_3N_4 appears as aggregated particles containing a nano sheet like structure. After introducing V_2O_5,the VOCN-1 nanocomposite shows a narrower particle size distribution on the nanosheet layer. The tightly packed surface morphology of the composite particles is beneficial for the efficient charge carrier separation.[21] Fig. 5 shows the TEM images of VOCN-1 photocatalyst. Further, the TEM images of sample reveals the sheet structure of g-C_3N_4 with

an agglomeration of V_2O_5 nanoparticles on the surface of g-C_3N_4. The elemental analysis of g-C_3N_4, V_2O_5 and VOCN-1 were examined by energy dispersive x-ray spectroscopy (EDAX) and the results are shown in Fig. 6(a), (b) and (c), respectively. It is clearly seen from Fig. 6 that the g-C_3N_4 is composed of carbon and nitrogen only and the V_2O_5 consists of V and O elements only and no other impurities are found. The weight and atomic percentages of species detected by EDAX are shown in Fig.6 inset. EDAX spectrum confirmed that the VOCN-1 nanocomposites consist of C, N, V and O elements.

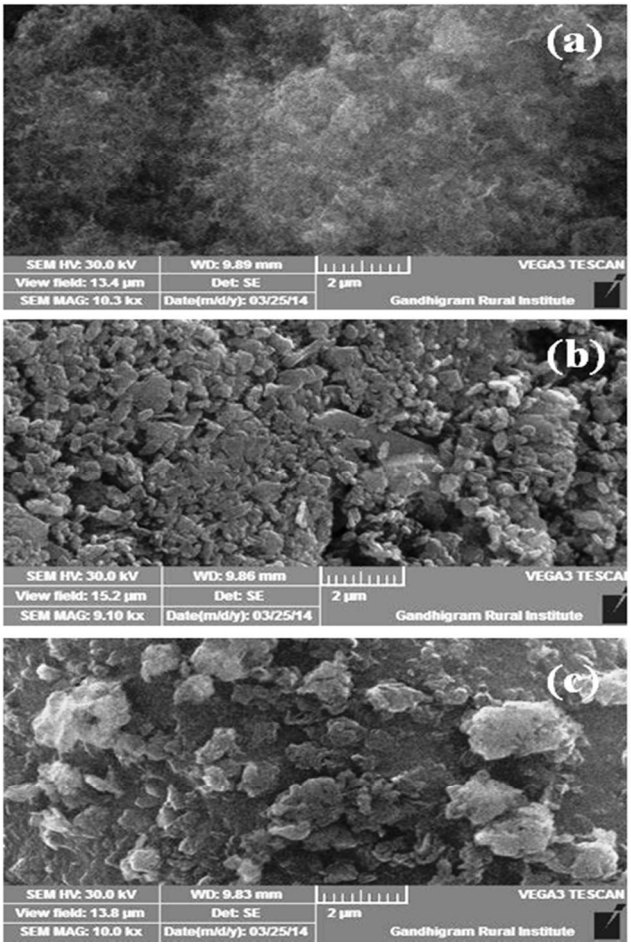

Fig. 4 Typical SEM images of (a) g-C_3N_4, (b) $V_2O_5$and (c) VOCN-1.

3.5 Photocatalytic activity of V_2O_5, g-C_3N_4 and V_2O_5/g-C_3N_4

The visible light photocatalytic activities of the V_2O_5, g-C_3N_4 and V_2O_5/g-C_3N_4 materials were evaluated from the photodegradation of DR81. It can be seen that the adsorption equilibrium between the catalyst and dye was reached after 90 min in the dark for all photocatalysts. A blank test in the absence of any catalyst was carried out for the dye alone ($5x10^{-5}$ M) for about 2 hours ofvisible light irradiation. There was no significant change inabsorbance of DR81 indicatingthe photostabilityof the dyeunder light irradiation (Fig.S1 of the ESI). The photodegradation

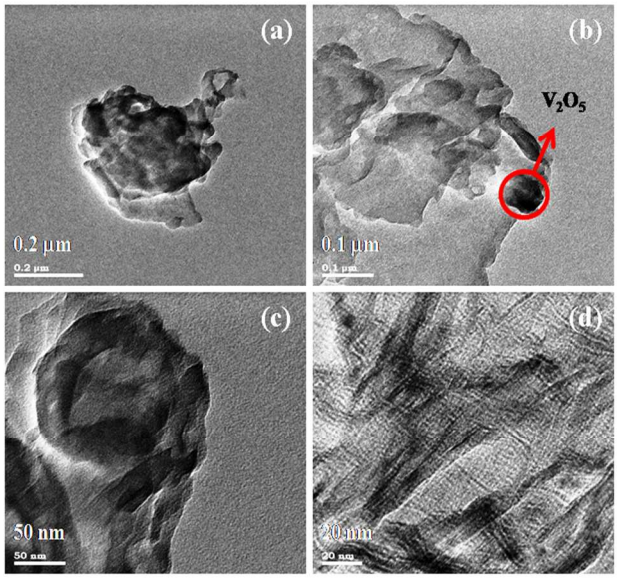

Fig. 5(a-d) TEM images of VOCN-1 photocatalyst particles.

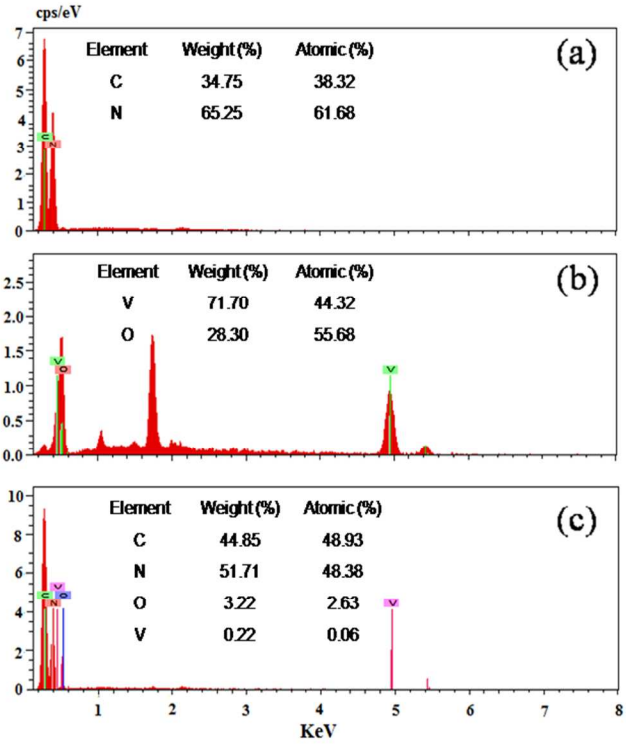

Fig. 6 EDAX spectra of (a) g-C_3N_4, (b) V_2O_5 and (c) VOCN-1.

DR81 over V_2O_5, g-C_3N_4, and V_2O_5/g-C_3N_4 with different mole percent (1%, 2%and 3%) of V_2O_5 are shown in Fig. 7(a). It can be seen that there was no significant degradation observed when V_2O_5 was used as a photocatalyst. The narrow band gap of V_2O_5 (2.64 eV) couldmake it active in a wide range of visible-light region but the rapid electron-hole pair recombination lowers the activity of V_2O_5 under both the ultraviolet and visible lights.[24,30] However, pure g-C_3N_4 demonstrated a good photocatalytic activity for the degradation of DR81 that can be attributed to the moderate band gab and unique electronic structure of g-

C_3N_4.[31]Further, it is noted that the V_2O_5/g-C_3N_4 composite exhibited significantly higher photocatalytic activity than that of pure V_2O_5 and g-C_3N_4, which indicates that the V_2O_5 plays an important role in the enhancement of DR81 degradation. These higher photocatalytic activities of composite indicated that the trapping sites of carriers are increased in V_2O_5/g-C_3N_4 photocatalysts. The highest photocatalytic activity was obtained for the 1 mole% loaded V_2O_5 to g-C_3N_4 (VOCN-1). However, with further increase of V_2O_5 content, photodegradation rate was decreased and it can be attributed to the fact that the excess of V_2O_5 species in the composite may act as a recombination center of electrons and holes that covers the active sites on the g-C_3N_4 surface.[13,32] The effect of VOCN-1 quantity (0.5, 1.0 and 1.5 g/L) on the photocatalytic degradation of DR81 were also studied and the results are shown in Fig. 7(b). It can be observed that the photodegradation rate increases with an increase in the catalyst loading. The reason for the observed trend is the increased availability of surface area and as well as the active sites of the catalyst.

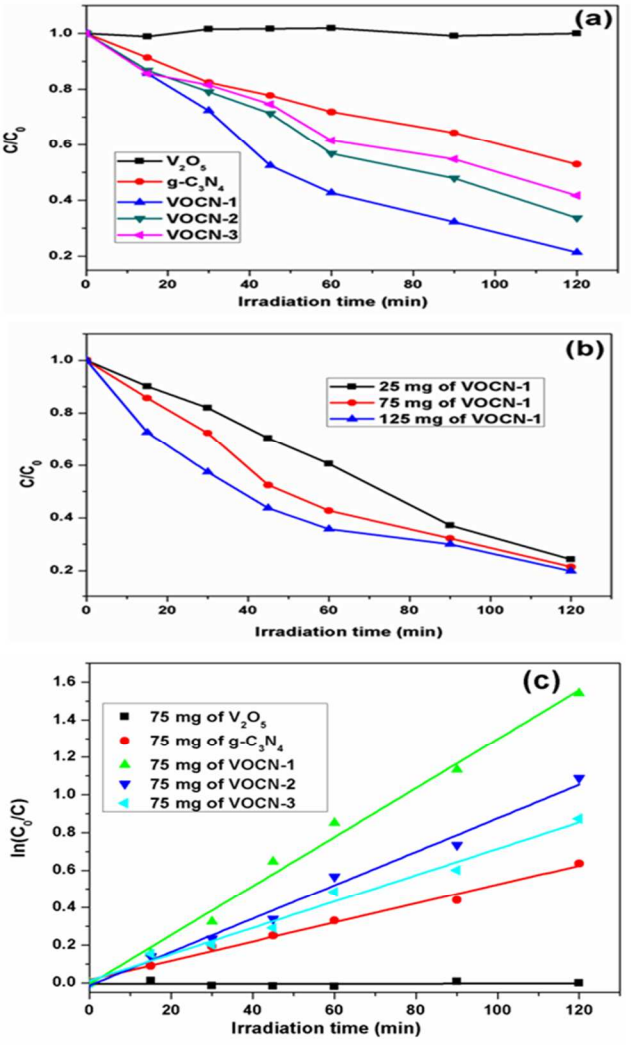

Fig. 7 (a)Photocatalytic degradation of DR81 over pure V_2O_5, g-C_3N_4 and V_2O_5/g-C_3N_4 photocatalysts under visible light irradiation, (b) Photocatalytic degradation of DR81 over different amounts (0.5, 1.0 and 1.5 g/L) of VOCN-1 and (c) First-order kinetics plots for the photodegradation of DR81 over pure V_2O_5, g-C_3N_4 and V_2O_5/g-C_3N_4 photocatalysts.

The photocatalytic degradation process was fitted to first-order kinetics and the rates were estimated based on the following equation.

$$\ln C_0/C = kt \qquad \text{---------(1)}$$

where k is the first-order rate constant (min^{-1}), t is the irradiation time (min), C_0 and C are the initial concentration and the concentration of DR81 at regular time intervals, respectively. The plot of $\ln(C_0/C)$ against the irradiation time (t) is shown in Fig. 7(c). The first order kinetics was confirmed from the linearity of ln C/Co vs time plot.

The stability of the photocatalyst is very important for its practical applications. To evaluate the photocatalytic stability of VOCN-1, repeated experiments for degradation of DR81 over VOCN-1 were performed and the results are shown in Fig. 8. It could be seen after 3 cycles, that the photocatalytic activity of VOCN-1 is remained at 75% of its first cycle. This implies the stability of VOCN-1 catalyst.

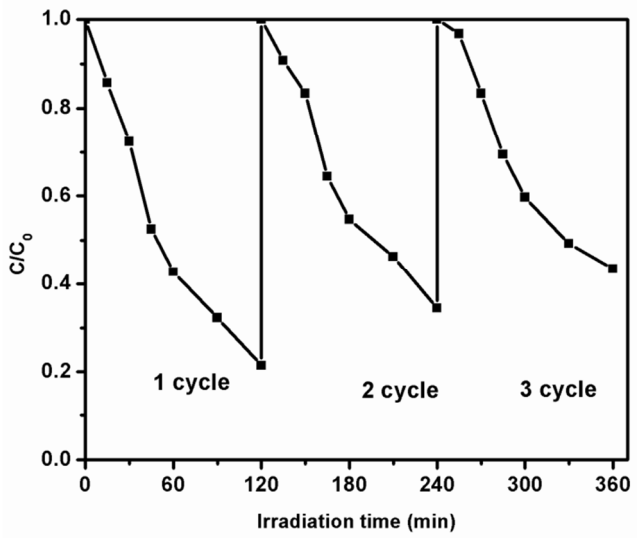

Fig. 8 Recyclability test of VOCN-1 for the degradation of DR81 under visible light irradiation.

3.6 Photoluminescence studies

The photoluminescence (PL) spectra of the synthesized photocatalysts are shown in Fig. 9. It can be seen that the PL intensity was increased on introducing of V_2O_5 to g-C_3N_4. The PL intensity of VOCN-1 catalyst increased and this enhancement may be attributed to the promotion of base functionalities ing-C_3N_4.[14,33] Generally, the lower PL intensity of photocatalysts corresponds to the higher photocatalytic efficiency because of efficient charge carrier separation and lower recombination rate. But V_2O_5/g-C_3N_4 composites showed special properties of enhanced photoluminescence due to the strong coupling of V_2O_5 with g-C_3N_4, which suggests that the V_2O_5/g-C_3N_4 composite may be a good candidate for potential applications such as luminescence and phosphorescence materials. The main emission peak is centered at 462 nm for the pure g-C_3N_4 and the peak position of the composite photocatalysts was similar to g-C_3N_4. However, the intensity of emission peak for V_2O_5/g-C_3N_4 composite was significantly increased. The VOCN-1 sample showed the strongest intensity. This result clearly reveals the

strong coupling of V_2O_5 and g-C_3N_4. However, the actual reason for the observed PL trend needs further investigation.

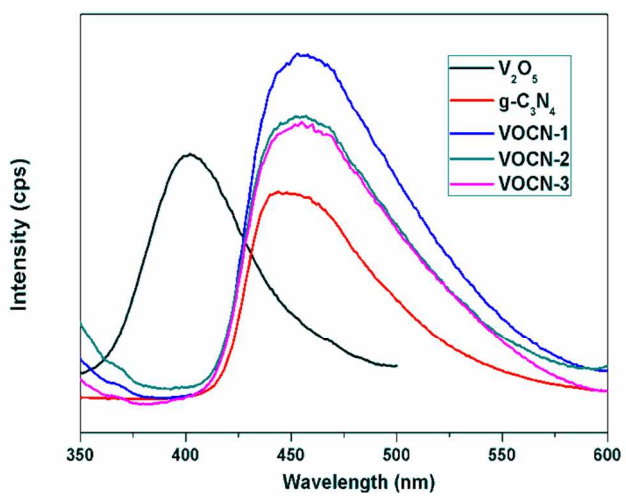

Fig. 9 Photoluminescence spectra of the synthesized photocatalysts.

3.7 Transient photocurrent and EIS study

The photoelectrochemical study was carried out for the bulk g-C_3N_4 and VOCN-1 to understand the electronic interaction between V_2O_5 and g-C_3N_4. The transient photocurrent response is recorded for light on-off cycles under visible light irradiation and the results are shown in Fig. 10(a). It should be noted that the photocurrent of VOCN-1 is much higher than that of g-C_3N_4. This result reveals that the VOCN-1 composite shows a better electron transfer rate than g-C_3N_4 and this may be the reason for the higher photocatalytic activity of VOCN-1 than the pure V_2O_5 and g-C_3N_4.

Electrochemical impedance spectroscopy (EIS) of the bulk g-C_3N_4 and VOCN-1 was investigated to know the interfacial electron transfer rate. The EIS data is presented as Nyquist plots for the g-C_3N_4 and VOCN-1 (Fig. 10(b)). The reaction rate occurring on the surface of the electrode is reflected by the radius of the arc on the Nyquist plots.[34] It was found that the arc radius of VOCN-1 is smaller than that of bulk g-C_3N_4. The smaller arc radius on Nyquist impedance plot of VOCN-1 indicates a more effective separation efficiency of photoinduced electron hole pairs and a faster interfacial charge transfer. Thus EIS study gives further support for the higher photocatalytic activity of VOCN-1.

3.8 Photocatalytic degradation mechanism

Based on the above experimental results, a possible photocatalytic mechanism has been proposed to explain the enhanced photocatalytic activity of the as-synthesized V_2O_5/g-C_3N_4 for the photocatalytic degradation of DR81. The visible-light driven electron-hole separation and the transport of photogenerated charge carriers on V_2O_5/g-C_3N_4 nanocomposite are illustrated in Fig. 11. Theconduction band (CB) and valance band (VB) potentials of g-C_3N_4 and V_2O_5were calculated using the following equation.[3]

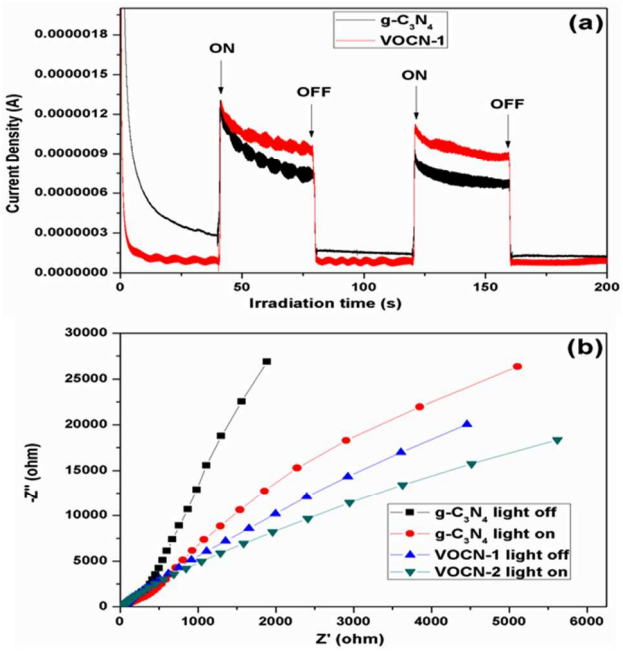

Fig. 10(a) Transient photocurrents of pure g-C_3N_4 and VOCN-1 under visible light irradiation, (b) Nyquist plots of pure g-C_3N_4 and VOCN-1 photocatalysts with and without visible light illumination.

$$E_{VB} = X - E^e + 0.5E_g \text{ ------} \quad (2)$$

$$E_{CB} = E_{VB} - E_g \text{ ------} \quad (3)$$

Where E_{VB} and E_{CB} are valance and conduction band potentials, X is the electronegativity of the semiconductor, E^e is the energy of free electrons on the hydrogen scale (~4.5 eV) and E_g is the band-gap energy of semiconductor. The absolute electronegativity of g-C_3N_4 and V_2O_5 is 4.73 and 6.10 eV.[35,36] The calculated CB and VB of g-C_3N_4 is -1.17 and 1.63 eV, whereas CB and VB of $V_2O_5$is 0.43 and 2.76 eV, respectively.The conduction band (CB) of g-C_3N_4 (-1.17) is more negative than that of V_2O_5 (0.43). Thus, the photogenerated electrons transfer from CB of g-C_3N_4 into that of V_2O_5, while the holes remain in the VB of g-C_3N_4. The photogenerated electrons and holes are easily separated in the transfer process, thereby enhancing the activity of photocatalyst for the degradation of DR81. The electron would subsequently transfer to the photocatalyst surface to react with water and oxygen to generate some active species such as hydroxyl radicals ($^{\cdot}OH$), superoxide radicals (O_2^{-}). These radicals are able to oxidize the pollutant due to their high oxidative capacities.[37-39]

The possible photocatalytic reactions (2-6) are similar to the reports available in the literature[32] and Fig. 11 shows the schematic illustration of the photocatalytic degradation of DR81 over V_2O_5-g-C_3N_4 photocatalyst under visible light irradiation.

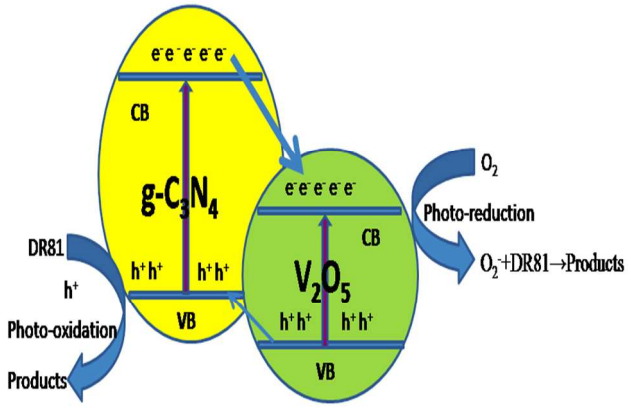

Fig. 11 Schematic illustration of the photocatalytic degradation mechanism of DR81 over V_2O_5/g-C_3N_4 under visible light irradiation.

$$V_2O_5/g\text{-}C_3N_4 \xrightarrow{\text{Visible light}} V_2O_5\,(e^-_{CB}) + g\text{-}C_3N_4\,(h^+)$$

$$V_2O_5\,(e^-_{CB}) + O_2 \longrightarrow O_2^-$$

$$O_2^- + 2\,e^-_{CB} + 2H^+ \longrightarrow {}^{\cdot}OH + OH^-$$

$$g\text{-}C_3N_4\,(h^+) + H_2O \longrightarrow H^+ + {}^{\cdot}OH$$

$$DR81 + {}^{\cdot}OH + O_2^- \longrightarrow \text{Degraded pollutants}$$

$$(CO_2, H_2O \textit{etc.})$$

4. Conclusions

New visible-light induced V_2O_5/g-C_3N_4 nanocomposite photocatalysts were successfully synthesized via wet-impregnation method using V_2O_5 and g-C_3N_4. The bulk V_2O_5 and g-C_3N_4 were synthesized from the heat treatment of citrate-vanadium complex and urea, respectively. A series of V_2O_5/g-C_3N_4 composites with different mole percent of V_2O_5 were synthesized. The phase purity interaction between the V_2O_5 and g-C_3N_4 in the composite was confirmed by various techniques, such as powder XRD, FT-IR, SEM, HRTEM and EDAX studies. The optical properties of photocatalysts with different mole% of V_2O_5 were examined by DRS and PL studies. The photocatalytic activity of V_2O_5/g-C_3N_4 nanocomposites is much higher than that of bulk V_2O_5 and g-C_3N_4 photocatalyst for the photodegradation of DR81. The enhancement of photocatalytic degradation is attributed to the efficient charge carrier separation of photoinduced electron and hole pairs. The optimal V_2O_5 content in the composite was found to be 1 mole%. The photoelectrochemical studies also confirmed the higher photocatalytic activity of VOCN-1. A possible photocatalytic mechanism has been proposed based on the photodegradation results. This work demonstrates that the V_2O_5/g-C_3N_4 composites are promising photocatalytic materials for efficient utilization of solar energy in environmental remediation applications.

Acknowledgements

We gratefully acknowledge the financial support received from Department of Atomic Energy-Board of Research in Nuclear Sciences (DAE-BRNS), Mumbai and Department of Science and Technology (DST), New Delhi, India.

Notes and references

[a] *Solar Energy Lab, Department of Chemistry, Thiruvalluvar University, Vellore-632 115, India. Fax: +91 416 2274748; Tel: +91 416 2274747; E-mail: jagan.madhavan@gmail.com(J. Madhavan)*

[b] *School of Chemistry, University of Melbourne, Parkville campus, Melbourne, VIC 3010, Australia.*

1 Y.F. Li, W.P. Zhang, X. Li, Y. Yu, *J. Phys. Chem. Solids* 2014, **75**, 86-93.
2 M.M. Mahlambi, O.T. Mahlangu, G.D. Vilakati,B.B. Mamba, *Ind. Eng. Chem. Res*., 2014, **53,**5709–5717.
3 J. Theerthagiri, R.A. Senthil, A. Priya, J. Madhavan, R.J.V. Michael, Muthupandian Ashokkumar, *RSC Adv.,* 2014, **4,** 38222-38229.
4 M. Aslam, I.M.I. Ismail, S. Chandrasekaran, A. Hameed, *J. Hazard. Mater.*, 2014, **276**, 120–128.
5 C. Zhao, H. Luo, F. Chen, P. Zhang, L. Yi, K. You, *Energy Environ. Sci.*, 2014, **7**, 1700-1707.
6 H. Zhou, l. Ding, T. Fan, J. Ding, D. Zhang, Q. Guo, *Appl. Catal. B: Environmental* 2014, **147**, 221-228.
7 S.K. Kansal, P. Kundu, S. Sood, R. Lamba, A. Umar, S.K. Mehta, *New J. Chem.*, 2014, **38**, 3220-3226.
8 S. Ma, J. Xue, Y. Zhou, Z. Zhang, *J. Mater. Chem. A* 2014, **2**, 7272-7280.
9 N. Soltani, E. Saion, W.M.M. Yunus, M. Erfani, M. Navasery, G. Bahmanrokh, K. Rezaee, *Appl. Surf. Sci.*, 2014, **290**, 440-447.
10 X.H. Guan, P. Qu, X. Guan, G.S. Wang, *RSC. Adv.*, 2014, **4**, 15579-15585.
11 Y. Du, L. Zhao, Y. Zhang, *J. Hazard. Mater.*, 2014, **267**, 55-61.
12 Y. He, L. Zhang, X. Wang, Y. Wu, H. Lin, L. Zhao, W. Weng, H. Wan, M. Fan, *RSC Adv.*, 2014, **4,** 13610-13619.
13 C. Han, L. Ge, C. Chen, Y. Li, X. Xiao, Y. Zhang, L. Guo, *Appl. Catal. B: Environmental* 2014, **147**, 546-553.
14 J. Shen, H. Yang, Q. Shen, Y. Feng, Q. Cai, *CystEngComm.*, 2014, **16**, 1868-1872.
15 F. Chang, Y. Xie, C. Li, J. Chen, J. Luo, X. Hu, J. Shen, *Appl. Surf. Sci.*, 2013, **280**, 967-974.
16 L. Shi, L. Liang, J. Ma, F. Wang, J. Sun, *Catal. Sci. Technol.*, 2014, **4**, 758-765.
17 J. Zhang, M. Zhang, S. Lin, X. Fu, X. Wang, *J. Catal.*, 2014, **310**, 24-30.
18 S. Kumar, A. Baruah, S. Tonda, B. Kumar, V. Shankar, B. Sreedhar, *Nanoscale* 2014, **6**, 4830-4842.
19 M. Shaloma, S. Inalb, D. Neherb, M. Antoniettia, *Catal. Today* 2014, **225**, 185-190.
20 K. Takanabe, K. Kamata, X. Wang, M. Antonietti,J. Kubota,K. Domen, *Phys. Chem. Chem. Phys.*, 2010, **12**, 13020-13025.
21 Y. Ji, J. Cao, L. Jiang, Y. Zhang, Z. Yi, *J. Alloys Compd.*, 2014, **590**, 9–14.
22 S. Chen, Y. Hu, S. Meng, X. Fu, *Appl. Catal. B: Environmental* 2014, **150-151**, 564-573.
23 D. Jiang, L. Chen, J. Xie, M. Chen, *Dalton Trans.*, 2014, **43**, 4878-4885.
24 A.A. Taha, A.A. Hriez, Y.N. Wu, H. Wang, F. Li, *J. Colloid Interface Sci.*, 2014, **417**,199-205.
25 L. Gao, X. Wang, L. Fei, M. Ji, H. Zheng, H. Zhang, T. Shen, K. Yang, *J. Cryst. Growth* 2005, **281**, 463-467.

26 Y. Tian, B. Chang, J. Fu, B. Zhou, j. Liu, F. Xi, X. Dong, *J. Solid State Chem.*, 2014, **212**, 1-6.

27 R. Abazari, S. Sanati, L.A. Saghatforoush, *Chem. Eng. J.*, 2014, **236,** 82-90.

28 F. Yang, V. Kuznietsov, M. Lublow, C. Merschjann, A. Steigert, J. Klaer, A. Thomas, T.S. Niedrig, *J. Mater. Chem. A* 2013, **1**, 6407-6415.

29 R. Saravanan, S. Joicy, V.K. Gupta, V. Narayanan, A. Stephen, *Mater. Sci. Eng. C* 2013, **33**, 4725-4731.

30 F. Chen, T.h. Wu, X.P. Zhou, *Catal. Commun.*, 2008, **9**, 1698-1703.

31 T. Li, L. Zhao, Y. He, J. Cai, M. Luo, J. Lin, *Appl. Catal. B: Environmental* 2013, **129**, 255-263.

32 S. Ye, L.G. Qiu, Y.P. Yuan, Y.J. Zhu, J. Xia, J.F. Zhu, *J. Mater. Chem. A* 2013, **1**, 3008-3015.

33 C.W. Zou, W. Gao, *Trans. Electr. Electron. Mater.*, 2010, **11**, 1-10.

34 H. Xu, J. Yan, X. She, L. Xu, J. Xia, Y. Xu, Y. Song, L. Huang, H. Li, *Nanoscale* 2014, **6**, 1406-1415.

35 W. Zhang, Y. Sun, F. Dong, W. Zhang, S. Duand, Q. Zhang, *Dalton Trans.,* 2014, **43**, 12026–12036.

36 F. Dong, Y. Sun, M. Fu, *Int. J. Photoenergy*, 2002, **569716**, 10.

37 F.T. Li, Y. Zhao, Q. Wang, X.J. Wang, Y.J. Hao, R.H. Liu, D. Zhao, *J. Hazard. Mater*., 2015, **283**, 371-381.

38 Y. Cui, J. Huang, X. Fu, X. Wang, *Catal. Sci. Technol*., 2012, **2**, 1396-1402.

39 S.C. Yan, Z.S. Li, Z.G. Zou, *Langmuir* 2010, **26**, 3894-3901

Synthesis of visible-light active V_2O_5/g-C_3N_4 heterojunction as an efficient photocatalytic and photoelectrochemical performance

Theerthagiri Jayaraman, Senthil Arumugam Raja, Annamalai Priya, Madhavan Jagannathan*, Muthupandian Ashokkumar

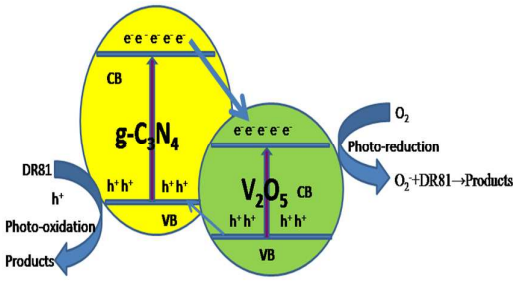

Synergistic enhancement in photocatalytic degradation of V_2O_5/g-C_3N_4 due to an increase in visible-light absorption efficiency and rapid photoinduced charge separation.